Diffraction-Unlimited Position Measurement of Ultracold Atoms in an Optical Lattice

Yuto Ashida[1] and Masahito Ueda[1,2]
[1]Department of Physics, University of Tokyo, 7-3-1 Hongo, Bunkyo-ku, Tokyo 113-0033, Japan
[2]RIKEN Center for Emergent Matter Science (CEMS), Wako, Saitama 351-0198, Japan
(Received 27 November 2014; published 26 August 2015)

We consider a method of high-fidelity, spatially resolved position measurement of ultracold atoms in an optical lattice. We show that the atom-number distribution can be nondestructively determined at a spatial resolution beyond the diffraction limit by tracking the progressive evolution of the many-body wave function collapse into a Fock state. We predict that the Pauli exclusion principle accelerates the rate of wave function collapse of fermions in comparison with bosons. A possible application of our principle of surpassing the diffraction limit to other imaging systems is discussed.

DOI: 10.1103/PhysRevLett.115.095301 PACS numbers: 67.85.-d, 03.65.Wj, 42.30.Wb

The classical theory of electromagnetism predicts that two objects with a distance less than a wavelength cannot be resolved [1]. This fundamental limit known as the diffraction limit has long imposed insurmountable constraints on optical physics. Recent achievements of the single-site resolved imaging [2,3] and addressing [4] of ultracold lattice gases are not exceptions: the diffraction limit requires a high numerical aperture lens and a large number of signals which forces us to use a near-resonant probe light which causes destruction of atomic states. As a result, all the experiments on single-site-resolved detection performed to date are destructive.

Quantum gases in an optical lattice offer an ideal playground to investigate strongly correlated systems and quantum information [5–7]. Recently, single-site resolved detection and addressing have emerged as a powerful tool for those studies [8–15]. Against such a backdrop, the development of a nondestructive measurement at the single-site level will have a significant impact on quantum simulation [16,17], quantum information processing [18,19], and open quantum many-body systems [20,21]. Furthermore, it will also be applied to the study of the influence of measurement backaction on quantum many-body states [22–26] and open up the possibility of generalizing the concepts in quantum feedback control [27,28] and quantum nondemolition (QND) measurement [29–31] to quantum many-body systems. To move toward these goals, there is an obvious need to develop methods which allow us to overcome the difficulty posed by the diffraction limit.

In this Letter, we propose a method that achieves this aim. We consider a quantum measurement of atomic positions in an optical lattice by spatially-resolved detections of dispersively scattered photons. A photodetection induces the many-body wave function collapse of atoms because a lens aperture diffracts the scattered field and imprints the spatial information of atoms on photons [32]. We show that the measurement backaction localizes the atom-number distribution and that tracking the progressive collapse into a Fock state enables us to perform diffraction-unlimited position measurement with near-unit fidelity. The main idea of our scheme of surpassing the diffraction limit is as follows. Since quantum measurement theory automatically takes into account Bayesian inference, we can extract the unbiased positional information of atoms and, remarkably, can precisely distinguish atomic configurations even if the diffraction limit is larger than the lattice constant. Previous works discussing nondestructive methods using off-resonant scattering with the angle-resolved measurement [33–38] and with the use of a cavity [39,40] could not achieve such a high spatial resolution. Furthermore, we find that the Pauli exclusion principle accelerates the rate of wave function collapse of fermions compared with bosons and, thus, our scheme is particularly suited for the recently realized single-site detection of fermionic gases [41–43].

While we here focus on atoms, our scheme can also be applied to other optical lattice systems such as single trapped ions [44–46]. Further, since the Bayesian analysis of the conditional probability distribution of source positions allows us to surpass the diffraction limit, our formulation may have an application to other imaging systems, e.g., photoactivated localization microscopy [47–52], as discussed later. We note that there also exist other approaches of overcoming the diffraction limit such as subwavelength-scale optical lattices using plasmons [53], photonic crystals [54], and running waves [55]. Other examples include stimulated emission depletion microscopy [56] and its coherent extension to magnetic imaging [57].

Model.—We consider two-level atoms in a lattice described by the many-body Hamiltonian

$$\hat{\mathcal{H}} = \int d^3r[\hat{H}_a(\mathbf{r}) + \hat{H}_{af}(\mathbf{r})] + \hat{H}_f, \tag{1}$$

where $\hat{H}_a(\mathbf{r}) = \sum_{i=g,e}\hbar\omega_i\hat{\Psi}_i^\dagger(\mathbf{r})\hat{\Psi}_i(\mathbf{r})$ is the Hamiltonian of atoms and $\hbar\omega_{g,e}$ are their ground (g) and excited (e) state

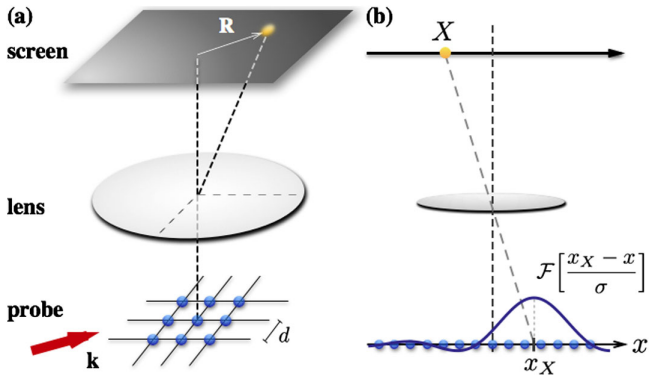

FIG. 1 (color online). Schematic geometry of our system. (a) Atoms trapped in an optical lattice are illuminated by an off-resonant probe light with wave vector $\mathbf{k}$. A scattered light is diffracted through a lens and detected on the screen. The position of a detected photon is denoted by $\mathbf{R}$. (b) A measurement backaction caused by the detection of a photon at position X. The many-body wave function shrinks according to the function $\mathcal{F}$ which peaks at x_X, where x_X is the lattice point diametrically opposite to X with respect to the center of the lens aperture.

energies, and $\hat{\Psi}_{g,e}(\mathbf{r})$ are the corresponding field operators; $\hat{H}_{af}(\mathbf{r}) = -(\mathbf{d}\cdot\hat{\mathbf{E}}(\mathbf{r})\hat{\Psi}_g^\dagger(\mathbf{r})\hat{\Psi}_e(\mathbf{r}) + \text{H.c.})$ describes the electric-dipole interaction with $\mathbf{d}$ and $\hat{\mathbf{E}}(\mathbf{r})$ being the electric dipole moment and the electric field operator, respectively; $\hat{H}_f = \sum_{\mathbf{k}',\sigma}\hbar\omega_{k'}\hat{a}^\dagger_{\mathbf{k}',\sigma}\hat{a}_{\mathbf{k}',\sigma}$ is the free-field Hamiltonian with $\hat{a}_{\mathbf{k}',\sigma}$ being the annihilation operator of a photon with wave vector $\mathbf{k}'$ and polarization σ. Atoms are illuminated by an off-resonant probe light whose positive frequency component is $\mathbf{E}_P^{(+)}(\mathbf{r}) = \mathbf{e}_P\mathcal{E}_0 e^{i\mathbf{k}\cdot\mathbf{r}}/2$. Each scattered photon is diffracted through a lens aperture and detected on a screen [see Fig. 1(a)]. We first focus on a 1D lattice and then discuss the generalization to a 2D lattice. In this Letter, we ignore tunneling of atoms through lattice potentials during imaging and focus on light scattering.

The scattered field can be calculated [58] by integrating out the Heisenberg equation of motion under the geometry as shown in Fig. 1. After performing the adiabatic elimination of the excited state and employing the tight-binding approximation, we arrive at the following expression of the scattered field at position X on the screen:

$$\hat{E}^{(+)}_{\text{sca}}(X) = \gamma\sum_m e^{-i\Delta\mathbf{k}\cdot md\mathbf{e}_x}\mathcal{F}\left[\frac{|x_X - md|}{\sigma}\right]\hat{b}_m^\dagger\hat{b}_m, \quad (2)$$

where the polarization vector is averaged out since we do not consider measuring the polarization of a photon, $\Delta\mathbf{k}$ is the wave-vector difference between incident and scattered photons, the operator $\hat{b}_m$ annihilates an atom at site m, x_X is the diagonal coordinate of the detected position [Fig. 1(b)], and $\mathcal{F}[y] \equiv J_1(y)/y$ which vanishes rapidly for $y \gg 1$. Here we assume that atoms remain in the lowest-band Wannier states during the imaging. This assumption should be met by using, for example, Raman sideband cooling [21,26,41,42], as discussed later. We introduce the parameter σ characterizing the resolution of the classical imaging method which is defined in terms of the numerical aperture of the lens N_A as $\sigma \equiv 1/kN_A$. The diffraction limit is usually characterized by the first zero of the Airy disk, $d_{\text{diff}} = 0.61(\lambda/N_A)$, which can be related to σ as $d_{\text{diff}} = 3.8\sigma$. Note that the classical imaging method can achieve the single-site resolved measurement only when the diffraction limit is comparable with the scale of the lattice constant $d_{\text{diff}} \lesssim d$.

Let us now consider the physical implication of Eq. (2). The measured observable can be continuously varied as we control the parameter σ by, for example, changing the distance between a lens and a lattice. When the lens is positioned at a far-field region and the numerical aperture is so low that σ is much larger than the lattice constant, the phase factor in Eq. (2) generates a Bragg diffraction pattern rather than the space-resolved imaging [59].

We develop a continuous quantum measurement theory and show that successive photodetections cause progressive collapse of the atomic state into a Fock state which, in turn, allows us to surpass the diffraction limit. We first consider an ideal situation in which the collection efficiency of scattered photons is unity and later discuss the effect of uncollected photons. Since the effective Hamiltonian commutes with the atom-number operator at each lattice site, the ideal photodetection of a dispersive scattered light constitutes a QND measurement of the atom-number statistics in the sense of Ref. [60]. Hence, our model presents a dual approach compared with a QND measurement [29–31] of the photon number by two-level atoms, where the photon number is determined by detecting the state of an output atom.

For the sake of concreteness, let us consider N atoms trapped in a 1D optical lattice with N_L sites. The state of a quantum gas is represented in terms of Fock states $|\{n_m\}\rangle \equiv |n_1,\ldots,n_{N_L}\rangle$ satisfying $\sum_{m=1}^{N_L} n_m = N$. Let ρ_0 be the density matrix for the initial motional state of atoms and $P_0[\{n_m\}]$ be the corresponding initial atom-number distribution. When we detect a photon at the screen position X, the change of the conditional state can be described by the measurement operator [Eq. (2)] as $\rho_0 \to \hat{E}^{(+)}_{\text{sca}}(X)\rho_0\hat{E}^{\dagger(+)}_{\text{sca}}(X)/\text{Tr}[\hat{E}^{(+)}_{\text{sca}}(X)\rho_0\hat{E}^{\dagger(+)}_{\text{sca}}(X)]$.

Suppose now that n photons were detected at the positions $\mathbf{X} \equiv \{X_1,\ldots,X_n\}$. Then the atom-number distribution of the quantum state becomes

$$P_n[\{n_m\}|\mathbf{X}] = \frac{P_0[\{n_m\}]\prod_{k=1}^n P[X_k|\{n_m\}]}{\sum_{\{n'_m\}}P_0[\{n'_m\}]\prod_{k=1}^n P[X_k|\{n'_m\}]}. \quad (3)$$

Here $P[X|\{n_m\}]$ is the conditional probability of detecting a photon at X, given that the atomic state is the Fock state $|\{n_m\}\rangle$:

$$P[X|\{n_m\}] = \frac{|\sum_{m=1}^{N_L} n_m \mathcal{F}[\frac{|x_X - md|}{\sigma}]|^2}{\int dX' |\sum_{m=1}^{N_L} n_m \mathcal{F}[\frac{|x_{X'} - md|}{\sigma}]|^2}, \quad (4)$$

where we neglect the contribution from the phase factor [58] in Eq. (2). We can track the progressive dynamics of the wave function collapse by applying Eq. (3) iteratively. The detection of a sufficiently large number of photons causes the state to collapse into a Fock state $|\{n_m\}\rangle$ and, hence, the occupied atom number at each lattice will be precisely determined. Note that the order of the measurement outcomes is irrelevant to the final collapsed state because all measurement operators commute with each other and only the accumulated histogram of the positional information of photodetections is sufficient to determine the final atom-number distribution. Nevertheless, tracking the progressive collapse in real time allows an adaptive measurement to terminate an imaging process once the required confidence level is attained so that unfavorable effects such as heating are kept minimal.

Let us here discuss why our method can surpass the diffraction limit. The crucial point is that since Eq. (3) derived from the quantum measurement theory automatically takes into account Bayesian inference, we can extract the detailed unbiased information about the positions of point sources. While the atomic configuration can also be inferred to some extent from an ordinary fitting procedure with a sufficiently large number of photodetections, our scheme achieves much better accuracy as detailed later.

Numerical simulations.—To illustrate the principle of surpassing the diffraction limit, we perform numerical simulations of our model. Figures 2(a) and 2(b), respectively, show the collapse of a bosonic state and that of a fermonic state into Fock states, where the initial state is chosen as a superposition of all possible Fock states. For comparison, we also show the histograms of detected positions of photons [Figs. 2(c) and 2(d)]. Our method enables us to distinguish between different Fock states by tracking the wave function collapse and hence, we can determine the atom number at each lattice site with near-unit fidelity beyond the conventional parity measurement. (For possible collision-induced loss, see the discussion below.) On the other hand, the classical diffraction-limited images [Figs. 2(c) and 2(d)] cannot resolve atoms placed at neighboring sites. The distribution of the collapsed states obtained by many realizations reproduces the initial state distribution.

To show the high fidelity of our scheme, we plot the confidence level of identifying the collapsed Fock state against the number of photodetections [Fig. 3(a)]. As shown, our scheme achieves a faster convergence to near unit fidelity than an ordinary fitting procedure. In particular, we find about an order of magnitude reduction in the required number of photodetections at 99.5% fidelity, which is the confidence level reported in Ref. [3]. We note that the regular analysis here based on the least squares fit also utilizes the same knowledge about the discrete positions in the lattice [61].

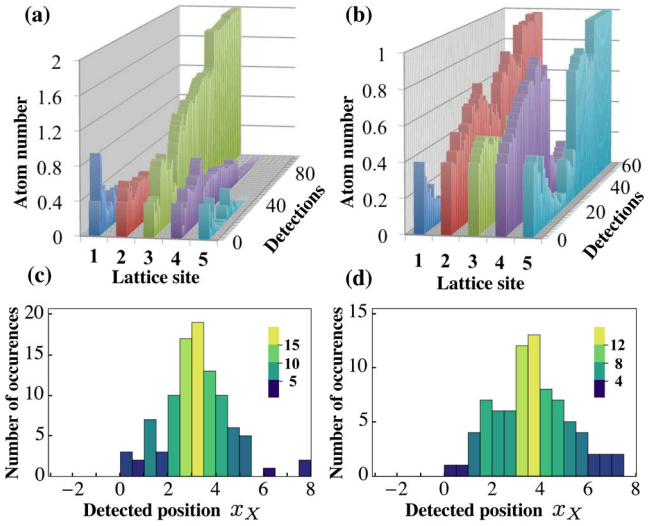

FIG. 2 (color online). Wave function collapse of atoms into Fock states [(a),(b)] and the diffraction-limited imaging signals [(c),(d)]. [(a),(b)] Successive detections of photons induce the state reduction of (a) bosons and that of (b) fermions into Fock states, with $N_L = 5$, $N = 2$, $\sigma = 1.0$ (in units of d). The atom number at each site is determined with near-unit fidelity by tracking the wave function collapse. [(c),(d)] The associated histograms of photodetection positions for (c) bosons and (d) fermions, respectively. Signals from atoms placed at different sites are substantially blurred by diffractions.

To investigate how quantum statistics of atoms affects the evolution of the wave function collapse, we plot the rate of wave function collapse against the resolution parameter σ [Fig. 3(b)]. We find that the rate of convergence is faster for fermions than bosons. This can be attributed to the Pauli exclusion principle which greatly reduces the number of

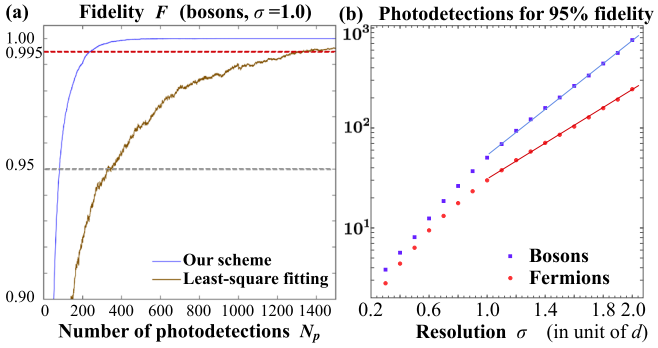

FIG. 3 (color online). Fidelity F and the required number of photodetections N_p for 95% fidelity. (a) The fidelity of our scheme (blue) compared with the result of the least-square fitting (yellow) for bosons at $\sigma = 1.0$. Dashed lines indicate 95% and 99.5% confidence level. (b) The number of photodetections required to achieve 95% fidelity (log-scale) plotted against the resolution σ for bosons (blue) and fermions (red), calculated for 10^4 realizations with $N_L = 5$ and $N = 2$.

possible configurations for fermions. Hence, our method is particularly suited for the single-site resolved detections of fermionic gases [41–43]. Another interesting feature is that the average number of photodetections needed to cause the many-body wave function collapse grows almost exponentially with the resolution parameter σ in a large-σ region. Because the rate of convergence can be related to the relative entropy of each measurement [62], this finding should have some information-theoretic background.

Asymptotic formula of the fidelity.—To explicitly show the efficiency of our scheme, here we discuss an analytical treatment of the confidence level. The fidelity F of identifying the collapsed Fock state can be asymptotically approximated by the following equation [62]:

$$F = 1 - \sum_{\{n_m\}} P_0[\{n_m\}] e^{-N_p R[\{n_m\}]}, \tag{5}$$

where N_p is the total number of photodetections and $R[\{n_m\}]$ is the minimal information-theoretic distance of the Fock state $\{n_m\}$:

$$R[\{n_m\}] \equiv \min_{\{n_k\} \neq \{n_m\}} D[P[X|\{n_m\}]|P[X|\{n_k\}]]. \tag{6}$$

Here $D[P_1|P_2]$ denotes the relative entropy between the two probability distributions P_1 and P_2. Equation (5) has the following physical meaning: the more distinguishable the interference patterns generated by different Fock states are, the faster the convergence to unit-fidelity is. From Eq. (5), one can calculate the expected fidelity for an arbitrary number of atoms and lattice sites. A scaling analysis of the error rate $\epsilon \equiv 1 - F$ implies that the fidelity scales mainly with the number of detections per atom (per lattice site) for fermions (bosons) [61].

As inferred from Eq. (5), an order-of-magnitude reduction of N_p [Fig. 3(a)] allows exponential improvement of the precision; i.e., the error rate of finding a particular Fock state becomes exponentially small. This is a particularly advantageous feature of the discretized space compared with the continuous space in which case only the square-root improvement of the precision is expected.

Experimental situations.—Let us make some practical considerations on the experimental implementation. First, we note that, in practice, only a portion of scattered photons can be collected and the back-action caused by destructions of uncollected photons in the far-field region also affects the dynamics of the wave function collapse [24,63]. In this case, Eq. (3) does not reconstruct an exact progressive dynamics of the wave function collapse. Nevertheless, the actual final collapsed Fock state, which is of primary interest, coincides with the one identified from Eq. (3) after a sufficient number of photodetections. As we pointed out earlier, the order of photodetection does not matter for the eventual collapsed wave function; this implies that the presence of uncollected photons only delays the speed of the collapse but not alter the eventual atomic state. Hence, our method can determine the atom distribution even in the presence of uncollected photons. In this respect, our formulation based on the Bayesian update of the conditional probability distribution of source positions may have an application to superresolved imaging of classical objects such as photoactivated localization microscopy [47–52].

Second, we note that our scheme can, in principle, be performed without prior knowledge of the total atom number [64,65]. This is because the relative entropy $D[P_{\mathrm{meas}}[X]|P[X|\{n_m\}]]$ between the measured photon-number distribution and the distribution from the collapsed Fock state provides a way of hypothesis testing of the atom number [61].

Third, we estimate a possible heating and show appropriate experimental parameters for our scheme. To this end, we consider the setup of Ref. [3]: $d = 532$ nm, $\lambda = 780$ nm and $N_A = 0.68$ (leading to $\sigma = 0.343$). Combining our numerical results of the required number of detections (about 5 detections per atom at $\sigma = 0.343$) with the experimental collection efficiency $\sim 10\%$, we obtain the total recoil energy as $\sim 93 E_r$ where $E_r \equiv \hbar^2\pi^2/2md^2$. Hence, the contribution of heating effects would be made negligible by, for example, implementing Raman sideband cooling as recently performed in Refs. [41,42]. To estimate the imaging time T_{img}, we consider the D_2 transition of ^{87}Rb [3] and the detuning $\Delta = 100\Gamma$, where $\Gamma/2\pi = 6.07$ MHz is the decay rate. From the required number of photodetections combined with the collection efficiency mentioned above, we obtain $T_{\mathrm{img}} \sim 9.6$ ms.

As for a possible loss of bosons due to light-assisted inelastic collisions, we note that usage of an off-resonant blue-detuned light can suppress such radiative losses [66]. To quantify the argument, we evaluate the inelastic scattering rate based on the Landau-Zener transition probability [66]. From the above experimental parameters combined with $\omega_{\mathrm{trap}}/2\pi = 20$ kHz for the harmonic trapping frequency of the optical lattice, we obtain 6×10^{-3} Hz as the inelastic collision rate per atom and hence, radiative losses can indeed be neglected in our consideration. We note that the Doppler heating effect can also be neglected because we consider large detuning. The crucial point is that, our method allows us to distinguish different Fock states with much less photons and thus without substantial heating which, in turn, allows the usage of a blue-detuned light. This contrasts with the conventional methods [2,3], which require use of a near-resonant red-detuned light to simultaneously achieve a high scattering rate and cooling atoms.

Finally, while reconstructing the collapse dynamics of a mesoscale number of atoms (typical in quantum gas microscope experiments [11–15]) is already within the scope of our model, one may need to reconstruct a macroscopic number of atoms, which, in practice, seems to be beyond the scope of our theory due to an exponential growth of computational cost. We note, however, that if the

final collapsed Fock state is of primary interest, one can avoid such problems by neglecting an intermediate process of the collapse [52].

Conclusion.—We have demonstrated that tracking the progressive evolution of the wave function collapse of a quantum many-body state provides a way to surpass the classical resolution limit, which—in contrast to the conventional diffraction-limited parity measurement—enables a nondestructive measurement of the atom-number distribution at the single-site level. Moreover, our principle of surpassing the diffraction limit has a much broader range of applications other than an optical lattice system and gives a powerful means of extracting positional information in different varieties of challenging situations.

We acknowledge I. Bloch, T. Fukuhara, R. Inoue, M. Miranda, and S. Nakajima for valuable discussions. This work was supported by KAKENHI Grant No. 26287088 from the Japan Society for the Promotion of Science, and a Grant-in-Aid for Scientific Research on Innovative Areas "Topological Materials Science" (KAKENHI Grant No. 15H05855), and the Photon Frontier Network Program from MEXT of Japan, and the Mitsubishi Foundation. Y. A. was supported by the Japan Society for the Promotion of Science through Program for Leading Graduate Schools (ALPS).

[1] M. Born and E. Wolf, *Principles of Optics* (Cambridge University Press, Cambridge, England, 1999).
[2] W. S. Bakr, J. I. Gillen, A. Peng, S. Fölling, and M. Greiner, Nature (London) **462**, 74 (2009).
[3] J. F. Sherson, C. Weitenberg, M. Endres, M. Cheneau, I. Bloch, and S. Kuhr, Nature (London) **467**, 68 (2010).
[4] C. Weitenberg, M. Endres, J. F. Sherson, M. Cheneau, P. Schauß, T. Fukuhara, I. Bloch, and S. Kuhr, Nature (London) **471**, 319 (2011).
[5] D. Jaksch, C. Bruder, J. I. Cirac, C. W. Gardiner, and P. Zoller, Phys. Rev. Lett. **81**, 3108 (1998).
[6] M. Lewenstein, A. Sanpera, V. Ahufinger, B. Damski, A. Sen, and U. Sen, Adv. Phys. **56**, 243 (2007).
[7] I. Bloch, J. Dalibard, and W. Zwerger, Rev. Mod. Phys. **80**, 885 (2008).
[8] W. S. Bakr, A. Peng, M. E. Tai, R. Ma, J. Simon, J. I. Gillen, S. Flling, L. Pollet, and M. Greiner, Science **329**, 547 (2010).
[9] J. Simon, W. S. Bakr, R. Ma, M. E. Tai, P. M. Preiss, and M. Greiner, Nature (London) **472**, 307 (2011).
[10] M. Endres, M. Cheneau, T. Fukuhara, C. Weitenberg, P. Schauß, C. Gross, L. Mazza, M. C. Bañuls, L. Pollet, I. Bloch, and S. Kuhr, Science **334**, 200 (2011).
[11] M. Cheneau, P. Barmettler, D. Poletti, M. Endres, P. Schauß, T. Fukuhara, C. Gross, I. Bloch, C. Kollath, and S. Kuhr, Nature (London) **481**, 484 (2012).
[12] T. Fukuhara, A. Kantian, M. Endres, M. Cheneau, P. Schauß, S. Hild, D. Bellem, U. Schollwöck, T. Giamarchi, C. Gross, I. Bloch, and S. Kuhr, Nat. Phys. **9**, 235 (2013).
[13] T. Fukuhara, P. Schausz, M. Endres, S. Hild, M. Cheneau, I. Bloch, and C. Gross, Nature (London) **502**, 76 (2013).
[14] P. M. Preiss, R. Ma, M. E. Tai, A. Lukin, M. Rispoli, P. Zupancic, Y. Lahini, R. Islam, and M. Greiner, Science **347**, 1229 (2015).
[15] T. Fukuhara, S. Hild, J. Zeiher, P. Schauß, I. Bloch, M. Endres, and C. Gross, Phys. Rev. Lett. **115**, 035302 (2015).
[16] I. Bloch, J. Dalibard, and S. Nascimbène, Nat. Phys. **8**, 267 (2012).
[17] I. M. Georgescu, S. Ashhab, and F. Nori, Rev. Mod. Phys. **86**, 153 (2014).
[18] K. D. Nelson, X. Li, and D. S. Weiss, Nat. Phys. **3**, 556 (2007).
[19] T. Byrnes, K. Wen, and Y. Yamamoto, Phys. Rev. A **85**, 040306 (2012).
[20] A. J. Daley, Adv. Phys. **63**, 77 (2014).
[21] Y. S. Patil, S. Chakram, L. M. Aycock, and M. Vengalattore, Phys. Rev. A **90**, 033422 (2014).
[22] S. Keßler, A. Holzner, I. P. McCulloch, J. von Delft, and F. Marquardt, Phys. Rev. A **85**, 011605 (2012).
[23] A. J. Daley, H. Pichler, J. Schachenmayer, and P. Zoller, Phys. Rev. Lett. **109**, 020505 (2012).
[24] J. S. Douglas and K. Burnett, Phys. Rev. A **86**, 052120 (2012).
[25] S. Keßler, I. P. McCulloch, and F. Marquardt, New J. Phys. **15**, 053043 (2013).
[26] Y. S. Patil, S. Chakram, and M. Vengalattore, arXiv: 1411.2678.
[27] H. Wiseman and G. Milburn, *Quantum Measurement and Control* (Cambridge University Press, Cambridge, England, 2010).
[28] C. Sayrin, I. Dotsenko, X. Zhou, B. Peaudecerf, T. Rybarczyk, S. Gleyzes, P. Rouchon, M. Mirrahimi, H. Amini, M. Brune, J.-M. Raimond, and S. Haroche, Nature (London) **477**, 73 (2011).
[29] M. Brune, S. Haroche, V. Lefevre, J. M. Raimond, and N. Zagury, Phys. Rev. Lett. **65**, 976 (1990).
[30] C. Guerlin, J. Bernu, S. Delèglise, C. Sayrin, S. Gleyzes, S. Kuhr, M. Brune, J.-M. Raimond, and S. Haroche, Nature (London) **448**, 889 (2007).
[31] T. Rybarczyk, S. Gerlich, B. Peaudecerf, M. Penasa, B. Julsgaard, K. Moelmer, S. Gleyzes, M. Brune, J.-M. Raimond, S. Haroche, and I. Dotsenko, arXiv:1409.0958.
[32] M. Holland, S. Marksteiner, P. Marte, and P. Zoller, Phys. Rev. Lett. **76**, 3683 (1996).
[33] J. Javanainen, Phys. Rev. Lett. **75**, 1927 (1995).
[34] J. Javanainen and J. Ruostekoski, Phys. Rev. A **52**, 3033 (1995).
[35] Z. Idziaszek, K. Rzążewski, and M. Lewenstein, Phys. Rev. A **61**, 053608 (2000).
[36] A. M. Rey, P. B. Blakie, G. Pupillo, C. J. Williams, and C. W. Clark, Phys. Rev. A **72**, 023407 (2005).
[37] K. Łakomy, Z. Idziaszek, and M. Trippenbach, Phys. Rev. A **80**, 043404 (2009).
[38] J. S. Douglas and K. Burnett, Phys. Rev. A **84**, 033637 (2011).
[39] I. B. Mekhov, C. Maschler, and H. Ritsch, Nat. Phys. **3**, 319 (2007).
[40] I. B. Mekhov and H. Ritsch, Phys. Rev. Lett. **102**, 020403 (2009).
[41] L. W. Cheuk, M. A. Nichols, M. Okan, T. Gersdorf, V. V. Ramasesh, W. S. Bakr, T. Lompe, and M. W. Zwierlein, Phys. Rev. Lett. **114**, 193001 (2015).

[42] M. F. Parsons, F. Huber, A. Mazurenko, C. S. Chiu, W. Setiawan, K. Wooley-Brown, S. Blatt, and M. Greiner, Phys. Rev. Lett. **114**, 213002 (2015).
[43] E. Haller, J. Hudson, A. Kelly, D. A. Cotta, P. Bruno, G. D. Bruce, and S. Kuhr, Nat. Phys., doi: (2015).
[44] D. Leibfried, R. Blatt, C. Monroe, and D. Wineland, Rev. Mod. Phys. **75**, 281 (2003).
[45] E. W. Streed, B. G. Norton, A. Jechow, T. J. Weinhold, and D. Kielpinski, Phys. Rev. Lett. **106**, 010502 (2011).
[46] A. Jechow, E. W. Streed, B. G. Norton, M. J. Petrasiunas, and D. Kielpinski, Opt. Lett. **36**, 1371 (2011).
[47] W. E. Moerner and L. Kador, Phys. Rev. Lett. **62**, 2535 (1989).
[48] R. M. Dickson, A. B. Cubitt, R. Y. Tsien, and W. E. Moerner, Nature (London) **388**, 355 (1997).
[49] E. Betzig, G. H. Patterson, R. Sougrat, O. W. Lindwasser, S. Olenych, J. S. Bonifacino, M. W. Davidson, J. Lippincott-Schwartz, and H. F. Hess, Science **313**, 1642 (2006).
[50] M. J. Rust, M. Bates, and X. Zhuang, Nat. Methods **3**, 793 (2006).
[51] S. J. Sahl and W. Moerner, Curr. Opin. Struct. Biol. **23**, 778 (2013).
[52] Y. Ashida and M. Ueda, arXiv:1505.00507.
[53] M. Gullans, T. G. Tiecke, D. E. Chang, J. Feist, J. D. Thompson, J. I. Cirac, P. Zoller, and M. D. Lukin, Phys. Rev. Lett. **109**, 235309 (2012).
[54] A. González-Tudela, C.-L. Hung, D. E. Chang, J. I. Cirac, and H. J. Kimble, Nat. Photonics **9**, 320 (2015).
[55] S. Nascimbene, N. Goldman, N. R. Cooper, and J. Dalibard, arXiv:1506.00558.
[56] T. A. Klar, S. Jakobs, M. Dyba, A. Egner, and S. W. Hell, Proc. Natl. Acad. Sci. U.S.A. **97**, 8206 (2000).
[57] D. Le Sage, K. Arai, D. R. Glenn, S. J. DeVience, L. M. Pham, L. Rahn-Lee, M. D. Lukin, A. Yacoby, A. Komeili, and R. L. Walsworth, Nature (London) **496**, 486 (2013).
[58] See Supplemental Material at http://link.aps.org/supplemental/10.1103/PhysRevLett.115.095301 for the derivation of the expression of the electric field and the conditional probability distribution.
[59] C. Weitenberg, P. Schauß, T. Fukuhara, M. Cheneau, M. Endres, I. Bloch, and S. Kuhr, Phys. Rev. Lett. **106**, 215301 (2011).
[60] V. B. Braginsky and F. Y. Khalili, Rev. Mod. Phys. **68**, 1 (1996).
[61] See Supplemental Material at http://link.aps.org/supplemental/10.1103/PhysRevLett.115.095301 for some technical details.
[62] M. Bauer and D. Bernard, Phys. Rev. A **84**, 044103 (2011).
[63] A. V. Rau, J. A. Dunningham, and K. Burnett, Science **301**, 1081 (2003).
[64] M. Karski, L. Förster, J. M. Choi, W. Alt, A. Widera, and D. Meschede, Phys. Rev. Lett. **102**, 053001 (2009).
[65] A. N. Wenz, G. Zrn, S. Murmann, I. Brouzos, T. Lompe, and S. Jochim, Science **342**, 457 (2013).
[66] J. Weiner, *Cold and Ultracold Collisions in Quantum Microscopic and Mesoscopic Systems* (Cambridge University Press, Cambridge, England, 2003).